

Archived at the Flinders Academic Commons:

<http://dspace.flinders.edu.au/dspace/>

This is the publisher's copyrighted version of this article.

The original can be found at: <http://zoolstud.sinica.edu.tw/Journals/43.2/376.pdf>

© 2004 Zoological Studies

Published version of the paper reproduced here in accordance with the copyright policy of the publisher. Personal use of this material is permitted. However, permission to reprint/republish this material for advertising or promotional purposes or for creating new collective works for resale or redistribution to servers or lists, or to reuse any copyrighted component of this work in other works must be obtained from the publisher.

Hydrodynamic Disturbance and Zooplankton Swimming Behavior

Laurent Seuront^{1,2,3,*}, Hidekatsu Yamazaki¹ and Sami Souissi²

¹Ocean Ecosystem Dynamics Laboratory, Department of Ocean Sciences, Tokyo University of Fisheries, 4-5-7 Konan, Minato-ku, Tokyo 108-8477, Japan

²Ecosystem Complexity Research Group, Station Marine de Wimereux, Université des Sciences et Technologies de Lille, CNRS-UMR 8013 ELICO, BP 80, F-62930 Wimereux, France

³School of Biology, Flinders University, GPO Box 2100, Adelaide 5001, South Australia

(Accepted February 23, 2004)

Laurent Seuront, Hidekatsu Yamazaki, and Sami Souissi (2004) Hydrodynamic disturbance and zooplankton swimming behavior. *Zoological Studies* 43(2): 376-387. Using a novel experimental setup that generates a realistic range of turbulence intensities, we investigated (i) the ability of zooplankton organisms to swim against a gradient of turbulence, and (ii) the qualitative and quantitative nature of their swimming behavior after short-term exposure to different intensities of turbulence. We used the cladoceran, *Daphnia pulicaria*, and the calanoid copepod, *Temora longicornis*, as model animals. First, both species increased their escape reactions with increasing turbulence intensity. However, this effect was significantly lower in *T. longicornis*. Second, swimming speed generated to reach the light source exceeded the turbulent velocities by up to 4-fold in *D. pulicaria* and 14-fold in *T. longicornis*. The swimming patterns of *T. longicornis* indicated a strong adaptation of this species to highly turbulent environments. Fractal analysis showed that the complexity of the swimming paths of *D. pulicaria* increased with the intensity of turbulence, and that this species exhibited a hysteretic cycle of 3 to 5 min for recovery from the prior swimming behavior. The implications on our findings on zooplankton trophodynamics, including predation vulnerability, encounter rates, and sensorial arguments, are discussed. <http://www.sinica.edu.tw/zool/zoolstud/43.2/376.pdf>

Key words: Zooplankton, Behavior, Turbulence, Fractals, Intermittency.

Micro-scale turbulence is widely recognized as a major driving force in plankton dynamics (e.g., Marrasé et al. 1997). In particular, turbulent processes have salient effects on processes such as metabolic rates, predator-prey encounter rates, grazing rates, egg production, swimming behavior, and population dynamics (Saiz and Alcaraz 1992a b, Saiz et al. 1992, Kjørboe and Saiz 1995, Kjørboe 1997). More-recent results suggest that the swimming abilities of zooplankton allow them to overcome turbulent fluctuations (Yamazaki and Squires 1996, Schmitt and Seuront 2001 2002), making them independent of local turbulent fluctuations. On the other hand, there is an increasing amount of literature demonstrating that zooplankton swimming behavior is highly structured (Coughlin et al. 1992, Bundy et al. 1993, Brewer 1996, Jonsson and Johansson 1997, Dowling et

al. 2000, Schmitt and Seuront 2001 2002, Seuront et al. 2004a b), far from the standard random-walk hypothesis that basically states that the amplitude and the direction of successive displacements follow a Gaussian distribution.

A related question is whether or not turbulence intermittency affects zooplankton swimming behavior. It is now widely recognized that turbulence (measured as the kinetic energy dissipation rate, ε , m^2/s^3), while typically referred to in terms of average values in the literature (Peters and Marrasé 2000), highly varies in both intensity and duration. More specifically, the distribution of turbulence both spatially and temporally must be thought of as a few patches of high turbulence intensity within a wide range of low-intensity patches (Seuront 2001, Seuront et al. 2001). This intrinsic property of turbulence has nevertheless

*To whom correspondence and reprint requests should be addressed. Tel: 33-321992937. Fax: 33-321992901. E-mail: Laurent.Seuront@univ-lille1.fr / Laurent.Seuront@flinders.edu.au

seldom been taken into account in zooplankton behavioral studies. While the escape behaviors of copepods to various hydrodynamic disturbances have been widely described (e.g., Singarajah 1969, Fields and Yen 1997, Suchman 2000, Buskey et al. 2002), to our knowledge, only a few studies (Costello et al. 1990, Marrasé et al. 1990, Hwang et al. 1994) have investigated the effect of turbulence intermittency on zooplankton behavior, mainly in terms of the time course of foraging and escape behavior frequencies. None of those studies focused on the consequences of turbulence intermittency on zooplankton swimming behavior. This topic still remains widely unexplored.

The objectives of this work were to investigate these different effects of turbulence on zooplankton swimming behavior in 2 different but complementary empirical ways. First, we estimated the ability of zooplankton organisms to swim against a gradient of turbulence and towards a light source. Second, we qualitatively and quantitatively quantified the swimming behaviors after short-term exposures to different intensities of turbulence. Specific procedures were developed to simulate intermittent bursts of turbulence encountered by zooplankton organisms in the field. These experiments were conducted with the freshwater cladoceran, *Daphnia pulex*, and the marine calanoid copepod, *Temora longicornis*.

MATERIALS AND METHODS

Generating and measuring turbulence

The experimental device used for observing zooplankton behaviors, the “Zoo-Turbularium”, is a Plexiglas aquarium 100 cm long, 18 cm wide, and 28 cm high (Fig. 1) containing 45 L of filtered fresh water. Turbulence was generated by a hori-

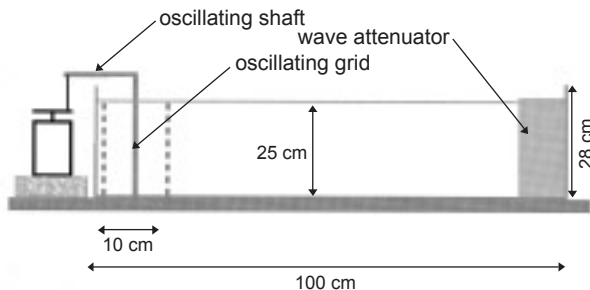


Fig. 1. Schematic illustration of the turbulence-generating apparatus, “Zoo-Turbularium”.

zontally sinusoidal oscillating grid, with a stroke of 10 cm centered 5.5 cm from the end wall of the tank, and driven by an electric motor. The free space between the grid and the side walls of the tank was $0.4 (\pm 0.1)$ mm, and the ratio of the open to the total area of the grid was 0.48 (holes were 16 cm^2 , i.e., $4 \times 4 \text{ cm}$, and bars were 0.9 cm thick). In order to limit reflections on the opposite end wall of the tank and to dampen the formation of waves, we placed a 10-cm-thick wave attenuator made of dense meshing of 2-mm-thick tubes of plastic on this end wall.

The turbulence intensities reported for the ocean range from $\varepsilon = 2.8 \times 10^{-11}$ to $4.7 \times 10^{-4} \text{ m}^2/\text{s}^3$ (Peters and Redondo 1997, Peters and Marrasé 2000). We were interested here (i) in the ability of zooplankton to swim against a gradient of turbulence, and (ii) in the effects of turbulence intermittency (i.e., strong bursts in the intensity of the kinetic energy dissipation rate, ε). Therefore, the oscillation frequency of the grid was adjusted so that it would generate turbulent dissipation rates ranging from medium to high intensities of turbulence encountered in the ocean, i.e., $\varepsilon \in (10^{-7}$ to $10^{-4} \text{ m}^2/\text{s}^3)$.

Dissipation rates in the tank were calculated from direct measurements of micro-scale velocities recorded with a 3-D acoustic Doppler velocimeter (ADV, Nortek). Velocity measurements were made at 4 different vertical positions (5, 10, 15, and 20 cm from the surface) and at 7 horizontal positions located every 10 cm, starting at 15 cm from the center of the stroke. For each horizontal position, 3 measurements were made: at the center of the tank and at a 4-cm distance from each wall. All measurements were made at a sampling interval of 0.04 s (25 Hz) for at least 90 s. Velocity measurements showed that mean velocities differed from 0 ($p < 0.05$, $n = 112$). These measurements indicated that there was residual circulation in the tank. The horizontal velocity was directed towards the grid in the lower part of the tank, while it was in the opposite direction in its upper part.

Estimates of dissipation rates, ε , were implicitly based on the hypothesis of isotropic, stationary turbulence (Taylor 1935, Tennekes 1975). In order to ensure the reliability of our dissipation rate estimates, we used time series of velocity deviations obtained by subtracting the mean velocity from instantaneous velocities. The resulting 3D velocity components, v_x , v_y , and v_z , were then used to estimate the root-mean-square turbulent velocity w from:

$$w = (v_x^2 + v_y^2 + v_z^2)^{1/2} \quad (1)$$

The energy dissipation rate, ε , was calculated following Taylor (1935):

$$\varepsilon = D \frac{w^3}{l}; \quad (2)$$

where D is a universal constant ($D=1$ following Stiansen and Sundby 2001), and l is the integral length scale of turbulence, i.e., a characteristic length scale representing larger turbulent vortexes. In order to account for the increase in l with distance from the grid, we used the empirical relationship (Thompson and Turner 1975):

$$l = k \times z; \quad (3)$$

where z is the distance from the center of the grid oscillation to the location of the measurement, and k is a proportionality constant ($k = 0.1$). Using 10, 20, and 30 strokes/min (referred to as turbulence levels 1, 2, and 3, hereafter), we obtained dissipation rates ranging from 3.8×10^{-8} to $4.8 \times 10^{-7} \text{ m}^2/\text{s}^3$, 8.7×10^{-8} to $8.5 \times 10^{-6} \text{ m}^2/\text{s}^3$, and 1.8×10^{-7} to $1.1 \times 10^{-4} \text{ m}^2/\text{s}^3$, respectively. The clear linear decrease in ε as a function of the distance from the grid is shown in a semilog plot (Fig. 2), which reveals an exponential decrease in turbulence behind the grid. At a given distance from the grid, there were no significant differences from 1 depth

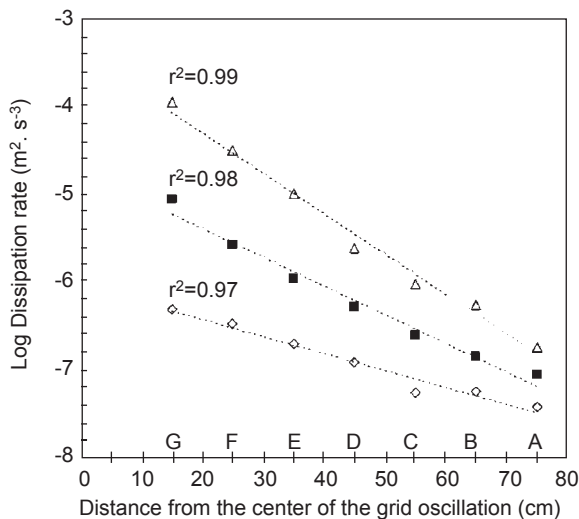


Fig. 2. Horizontal distribution of turbulent energy dissipation rates derived from acoustically measured 3-D micro-scale velocity fluctuations for 3 stroke frequencies of 10 (open rhombs), 20 (black squares), and 30 (open triangles) strokes/min as a function of the distance (cm) from the center of the grid oscillation. Letters refer to the 7 test areas investigated in this work (see text for further details).

to another, regardless of the grid frequency considered (Friedman test, $p > 0.05$). The turbulence levels defined here are characteristic of turbulent dissipation rates experienced by *Daphnia pulicaria* in surface waters of lakes and by *Temora longicornis* in its typical coastal water habitats (e.g., Seuront et al. 2002 2004a b).

Live material collection and acclimation

Daphnia pulicaria. All experiments were performed using a clone of *D. pulicaria* kept in an outside mesocosm culture by Prof. K. Sakai at the Tokyo Univ. of Fisheries, Japan. Individuals were collected from the mesocosm using a 2-L beaker, gently filtered through a 200- μm mesh sieve, and stored in a 25-L aquarium filled with mesocosm water at densities of around 50 individuals/L under ambient light conditions. Prior to the experiments, non-egg-bearing adult females (carapace length, $1.9 \pm 0.1 \text{ mm}$, $\bar{x} \pm \text{SD mm}$; $n = 240$) were sorted by pipette under a dissecting microscope, and acclimated for 12 h at 21°C in 5-L plastic buckets filled with 0.45- μm -filtered mesocosm water. All experiments were conducted at the Department of Ocean Sciences, Tokyo Univ. of Fisheries, in June 2000 in the "Zoo-Turbularium" filled with 45 L of 0.45- μm -filtered mesocosm water at 21°C .

Temora longicornis. Individuals of the copepod *Temora longicornis* were collected with a WP2 net (200- μm mesh) from the surface of tidally mixed inshore waters of the Eastern English Channel. Specimens were diluted in buckets with surface water and transported to the laboratory. The acclimation of copepods consisted of storage in 20-L beakers filled with natural seawater. Prior to the experiments, adult females (carapace length, $1.0 \pm 0.1 \text{ mm}$, $\bar{x} \pm \text{SD mm}$; $n = 240$) were sorted by pipette under a dissecting microscope, and acclimated for 12 h at 20°C in 0.45- μm -filtered seawater. All experiments were conducted at the Station Marine de Wimereux (France) in August 2001 in the "Zoo-Turbularium" filled with 45 L of 0.45- μm -filtered seawater at 20°C .

Experimental procedures and behavioral observations

Turbulence and zooplankton swimming ability. Because of the above-mentioned observed residual circulation within the "Zoo-Turbularium", we needed to keep zooplankton individuals within the upper part of the tank, and to make them swim

against this residual circulation. By considering the phototactic behavior of zooplankton organisms (e.g., Van Gool and Ringelberg 2002), we were able to achieve this by covering the upper and lower parts of the tank with opaque sheets of dark paper, and illuminating the upper part of the tank with a diffuse cold light placed sideways 0.25 m behind the grid; this resulted in illumination of about $12 \mu\text{E}/\text{m}^2/\text{s}$ in the vessel, which was approximately equal to full daylight. Note that this surface residual circulation corresponded to a gradient in the horizontal velocity generated by grid oscillations that ranged from 0.01 to 0.71 cm/s, 0.10 to 1.40 cm/s, and 0.15 to 1.70 cm/s for turbulence levels 1, 2, and 3, respectively.

To investigate the precise response of animals within these gradients, we divided the “Zoo-Turbularium” into 7 test sections 10 cm wide, centered on the 7 axial ADV measurement points, and numbered them from A to G, from the furthest to the closest measurement points with respect to the grid (Fig. 3). A single animal was then left in the tank, at 75 cm from the center of the stroke (i.e., the furthest end of the test area identified as “A” in Fig. 3). Using a computer-interfaced event recorder, we measured (i) the number of escape reactions (i.e., the number of swimming bouts not oriented towards the grid) and (ii) the time spent in each test area. This experimental procedure was conducted on both *D. pulicaria* and *T. longicornis*. Ten individuals were used for the non-turbulent reference treatments, for each turbulence level (3 turbulence levels), and each test area (7 test areas). The entire experiment thus consisted of 24 treat-

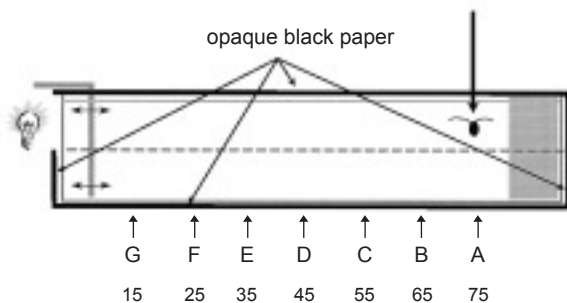


Fig. 3. Schematic illustration of the experimental setup designed to investigate the ability of *Daphnia pulicaria* and *Temora longicornis* to swim against a gradient of turbulence. Arrows refer to the center of each test area, related to the letters A to G. Numbers below the letters indicate the distance (cm) from the center of the grid oscillation. A single animal was left in the tank at 75 cm from the center of the stroke, and using a computer-interfaced event recorder, we measured (i) the number of escape reactions and (ii) the time spent in each test area.

ments and involved 240 individuals of *D. pulicaria* and 240 individuals of *T. longicornis*.

Turbulence intermittency and zooplankton swimming behavior. The objective of this experiment was to record the swimming behaviors of zooplankton individuals after a short exposure (1 min) to different intensities of turbulence. Tests were conducted at all 21 levels of dissipation rates as shown in fig. 2. The major challenge was then to keep the animals within areas of similar dissipation rates for 1 min. We covered the entire “Zoo-Turbularium” with opaque sheets of black paper except for a test area 10 cm wide (corresponding to a volume of 4.75 L), and centered on the axial ADV measurement points; this area was covered with white paper on the bottom and sides. The test area was illuminated with a diffuse cold light placed 0.5 m above the test unit. This resulted in illumination of $12 \mu\text{E}/\text{m}^2/\text{s}$ in the vessel, approximately equal to full daylight (Fig. 4). For this experiment, the different test areas (A to G) must be thought of as turbulent patches which zooplank-

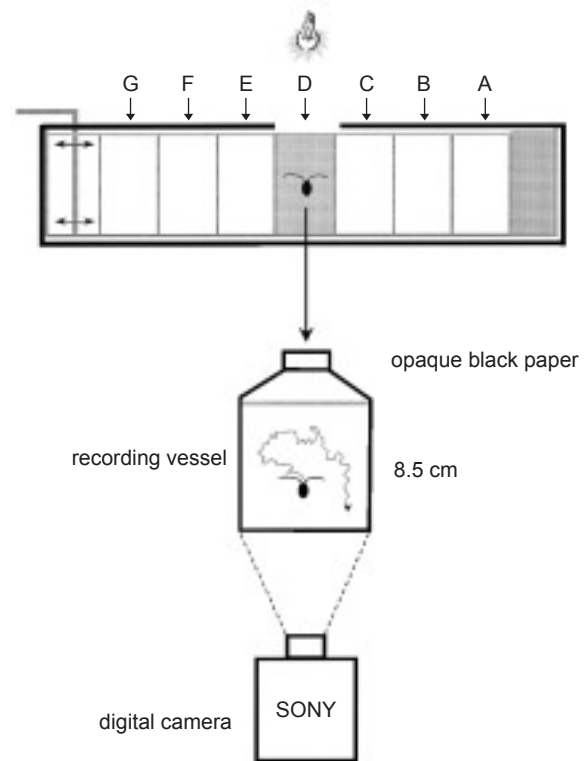


Fig. 4. Schematic illustration of the experimental setup to investigate the effect of turbulence intermittency on *Daphnia pulicaria* swimming behavior. A single animal was kept in an illuminated test area for 1 min, picked up in a recording vessel, and video-recorded for 5 min.

ton organisms might encounter while swimming.

A single animal was selected out by pipette and left in the test area for 1 min. All animals tested remained within the test areas. The animal was subsequently picked up, and left in a 217-ml (8.5 x 8.5 x 3 cm) Plexiglas recording vessel. Each individual was recorded swimming for 5 min using a digital camera (Sony Handycam, Japan) at a rate of 30 frames/s. In order to investigate the time course of the behavioral response to turbulence, videos were divided into 5 segments of 1 min each, after which valid segments were identified for analysis. Valid segments consisted of pathways in which the animals were freely swimming at least 2 body lengths away from any of the chamber's walls or the surface. Each level of turbulence was tested with 10 different individuals, and compared to the results obtained from 10 reference individuals that were not exposed to turbulence. These experiments were only conducted with the cladoceran, *Daphnia pulicaria*.

Quantifying zooplankton swimming behavior

Because traditional metrics used to characterize animal movements have been proven to be scale-dependent, we used fractal analysis which is based on the premise that the fractal dimension can serve as a scale-independent descriptor of the path an organism takes as it swims around (Seuront et al. 2004a). The philosophy behind fractals is as follows: if an organism moves along a completely linear path, then the actual distance traveled, L , equals the displacement between the start and the finish, δ . The relationship between these 2 variables is linear. In other words, if we assume a power law relating L to δ , i.e., $L^D = \delta$, then the exponent, D , is equal to 1. According to this power law, if the path deviates from linearity, i.e., it becomes curvilinear, the exponent will then be greater than 1. In the extreme example of curviness, i.e., for the case of Brownian motion in 2 dimensions, $D = 2$ (Mandelbrot 1983). It appears that D provides a measure of the path's "sinuosity", "tortuosity", or "complexity", with extreme cases delineated by linear and Brownian movement, respectively, and real-life cases expected to fall between these extremes.

More specifically, we estimated fractal dimensions using the box-counting method. Formally, the method finds the " λ cover" of the object, i.e., the number of pixels of length λ required to cover the object (Voss 1988). A more-practical alternative is to superimpose a regular grid of pixels of

length λ on the object and count the number of "occupied" pixels (Fig. 5). This procedure is repeated using different values for λ . The volume occupied by a path is then estimated with a series of counting boxes spanning a range of volumes down to some small fraction of the entire volume (Fig. 5). The number of occupied boxes increases with decreasing box size, leading to the following power-law relationship (Loehle 1990):

$$N(\lambda) = k \times \lambda^{-D}; \quad (4)$$

where λ is the box size, $N(\lambda)$ is the number of boxes occupied by the path, k is a constant, and D is the fractal dimension. D is estimated from the slope of the linear trend of the log-log plot of $N(\lambda)$ versus λ (Fig. 5).

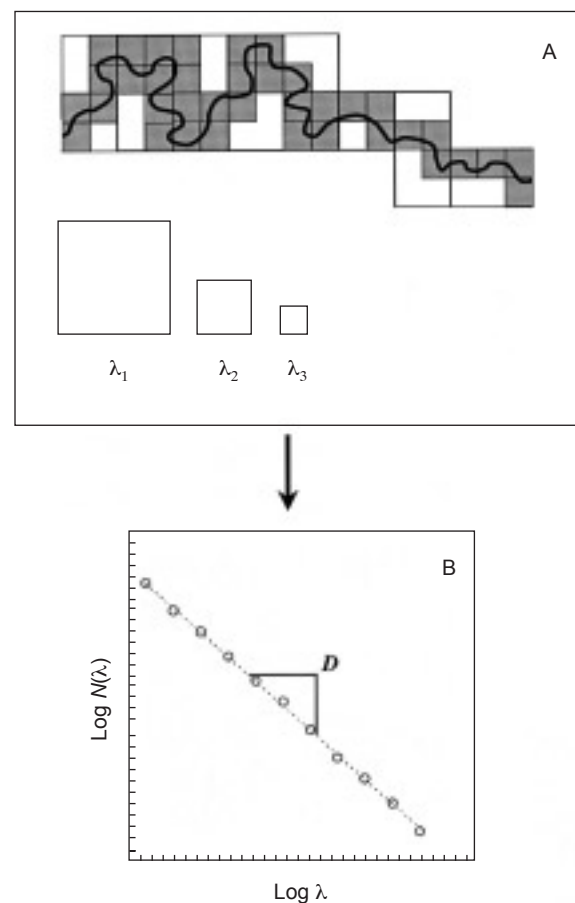


Fig. 5. Schematic illustration of the fractal characterization of a swimming path. The path was covered by a square of decreasing size, λ , and the occupied squares were counted (A). The number of occupied squares, $N(\lambda)$, was then plotted against the length scale, λ , in a log-log plot. The slope of the linear trend of $N(\lambda)$ vs. $\log \lambda$ provides the fractal dimension of the swimming path (B).

Statistical analyses

Because of the weak number of observations ($n = 10$) for both factors, the grid stroke frequency ($a = 3$) and the distance from the grid ($b = 7$), we based our analyses on non-parametric statistics. The effects of experimental factors (turbulence intensity and distance from the grid) on escape events, swimming speed, and fractal dimensions were thus investigated using the Scheirer-Ray-Hare extension of the Kruskal-Wallis test (Scheirer et al. 1976, Sokal and Rohlf 1995), referred to as the SRH test hereafter. Appropriate multiple comparison procedures were subsequently used to test for differences between the non-turbulent control and the 3 turbulent conditions, and the Jonckheere test for ordered alternatives was used to test for the presence of a gradient in observations conducted at different distances from the grid (Siegel and Castellan 1988).

RESULTS

Turbulence and zooplankton swimming ability

The escape responses of *Daphnia pulicaria* and *Temora longicornis* showed very distinct patterns (Fig. 6). For *D. pulicaria* (Fig. 6A), the number of escapes also significantly differed between the turbulence treatments and test areas (SRH test, $p < 0.05$). Multiple comparison procedures finally showed that the number of escapes was always significantly higher in turbulent than in non-turbulent conditions $p < 0.05$, and increased significantly when the distance from the center of the stroke decreased (Jonckheere test, $p < 0.05$). More specifically, the percentage of *Daphnia* individuals that exhibited escape responses increased significantly when the distance from the center of the grid stroke decreased, while the turbulence intensity increased at a given distance from the grid (Fig. 6B). In contrast, the number of escapes observed for *T. longicornis* exhibited no significant differences related to the distance from the center of the grid stroke, or according to the turbulence intensities (SRH test, $p > 0.05$; Fig. 6C). However, the percentages of *Temora* individuals that exhibited an escape reaction showed a pattern similar to that observed for *Daphnia*, but it never reached 100% and increased with decreasing distance

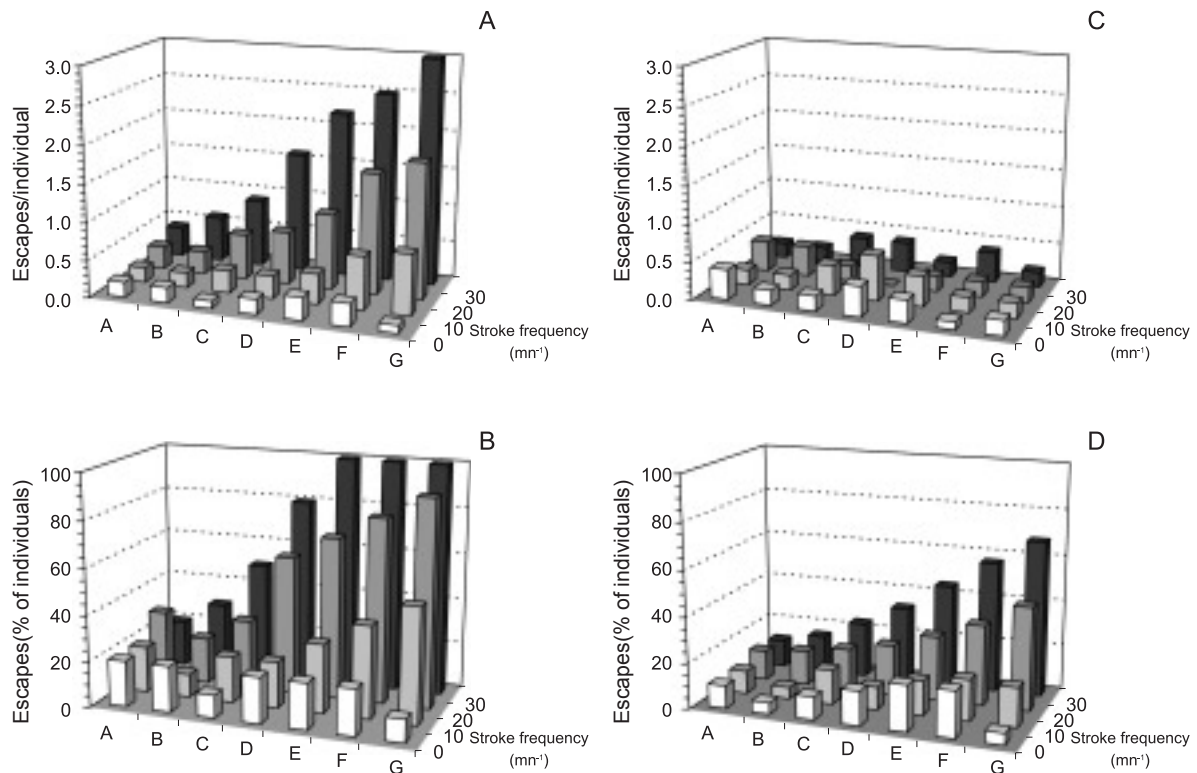


Fig. 6. Escape reactions of *Daphnia pulicaria* (A, B) and *Temora longicornis* (C, D) within the 7 test areas in non-turbulent conditions and for 3 levels of turbulence. The mean number of escape reactions per individual (A, C) and the percentage of individuals exhibiting escape reactions (B, D) are shown. Ten individuals of *D. pulicaria* and *T. longicornis* were considered for each experimental condition.

from the grid only for the 2 highest levels of turbulence (Fig. 6D).

The swimming mean speed of *D. pulex* significantly increased with decreased distance from the grid for both still and turbulent treatments (Jonckheere test, $p < 0.05$; Fig. 7A). The subsequent effective speed (i.e., the sum of the observed swimming speeds and the norm of the horizontal component of the turbulent velocity), showed significant increases for all turbulent treatments with decreased distance from the grid

(Jonckheere test, $p < 0.05$; Fig. 7B). The increase in swimming speed was then bounded between 9% and 390% (Fig. 7C). The situation greatly differed in the case of *T. longicornis*. The mean swimming speeds were constant regardless of the treatment or the distance from the grid (SRH test, $p < 0.05$; Fig. 7D). The effective speed then simply reflected the behavior of the horizontal components of the turbulent velocity. It showed significant increases with decreased distance from the grid and with increased turbulence for most dis-

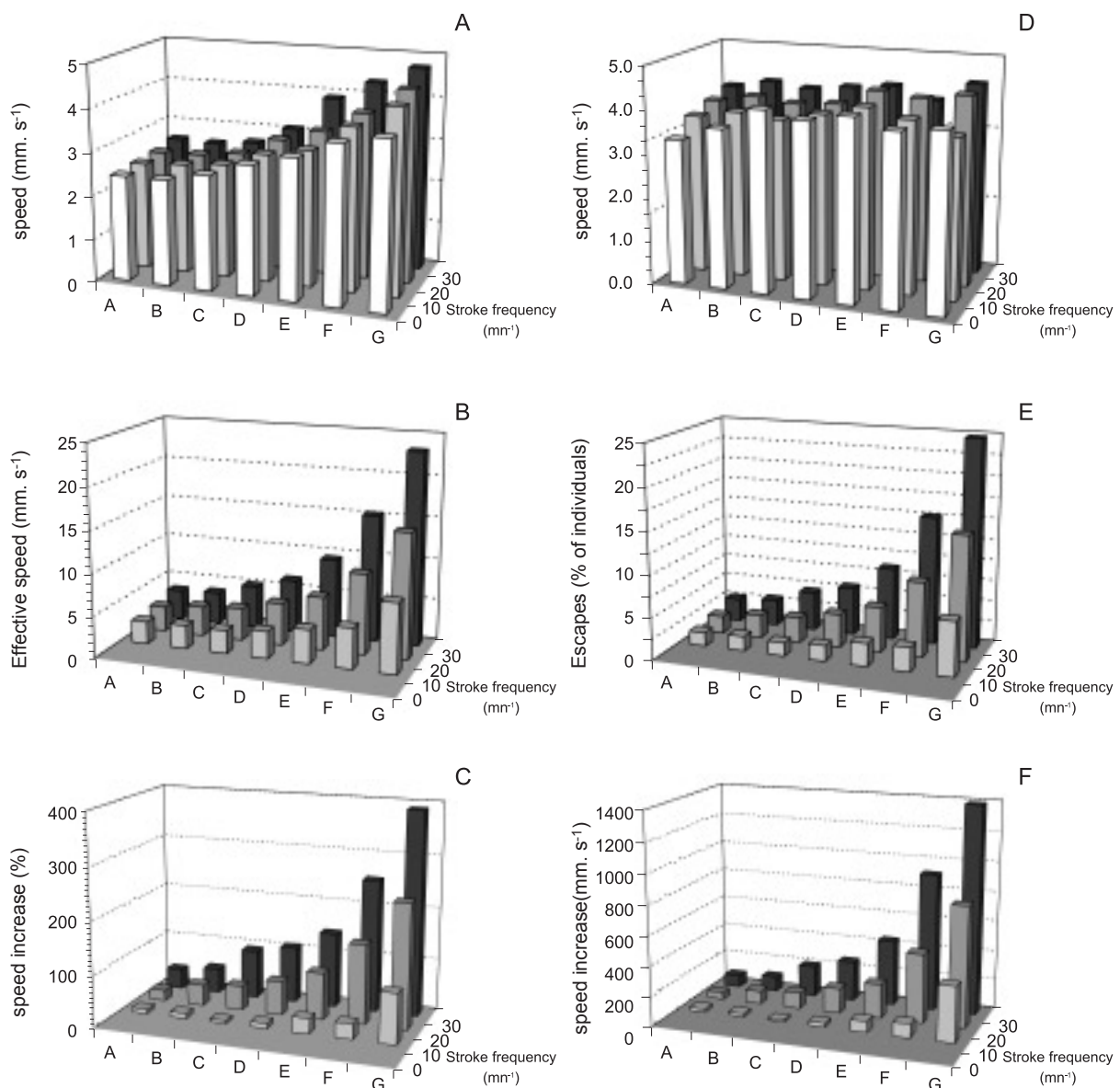


Fig. 7. Mean speed (mm/s; A, D), mean effective speed (mm/s; B, E), and percentage of the increase between swimming and effective swimming speeds (C, F) for *Daphnia pulex* (A~C) and *Temora longicornis* (D~F). Ten individuals of *D. pulex* and *T. longicornis* were considered for each experimental condition.

tances from the grid (Fig. 7E). Finally, the increase in swimming speed was considerable, ranging from 20% for the smallest level of turbulence and the largest distance from the grid to 1400% for the highest level of turbulence and the smallest distance from the grid (Fig. 7F).

Turbulence intermittency and zooplankton swimming behavior

Samples of trajectories recorded in still conditions and after a 1-min exposure to turbulence level 1 are shown in fig. 8. Note the linear character of the trajectory in still water conditions (Fig. 8A) when compared to the turbulent one which was more complex and curvy (Fig. 8B). The fractal dimensions estimated from the trajectories of *D. pulicaria* kept in still water conditions, $D = 1.16 \pm 0.02(\bar{x} \pm \text{SD})$; referred to as “still fractal dimensions” hereafter), showed no significant differences related to their position within the “Zoo-Turbularium” nor to the duration of the observations after their transfer to the recording vessel (Friedman test, $p > 0.05$; Fig. 9A). Results obtained from the experiments conducted at the 3 different turbulence levels were more complex. First, the fractal dimensions, D , estimated from the trajectories recorded during the 1st minute after turbulence exposure were significantly higher than those under still conditions (Friedman test, $n = 2$, $p < 0.05$, and subsequently, the Jonckheere test, $p < 0.05$) for all test areas, except areas A to D for turbulence level 1, and areas A to C for turbulence levels 2 and 3. These fractal dimensions then reached 1.36 ± 0.03 , 1.44 ± 0.04 , and 1.55 ± 0.05 in test area G for turbulence levels 1, 2, and 3, respectively. Second, the time course of the fractal dimensions, D , showed that the still fractal dimensions recovered within 3 to 5 min following turbulence exposures (Fig. 9B~D). More specifically, the higher

the fractal dimensions observed after turbulence exposure, the longer it took to recover to the reference behavior.

DISCUSSION

Fractal versus multifractal behavioral analyses

In recent contributions, it has been shown that the swimming behavior of zooplankton organisms can also be characterized in terms of multifractals (Schmitt and Seuront 2001 2002, Seuront et al. 2004b). To avoid misinterpretations, one must note that fractal and multifractal frameworks are fully compatible, the choice of a method being a matter of convenience or dependent on the specific objectives of the study. The fractal behavioral approach introduced here and elsewhere (e.g., Coughlin et al. 1992, Bundy et al. 1993, Jonsson and Johansson 1997, Dowling et al. 2000, Seuront et al. 2004a) is intrinsically based on the geometric properties of a swimming path, in terms of space-filling properties. A simple, smooth, quasi-linear path is thus characterized by a low fractal dimension ($D \rightarrow 1$), while that of a more-tortuous path is higher, ultimately reaching the maximum space-filling value of $D = 2$. Alternatively, the multifractal approach is a stochastic generalization of the fractal approach, leading to characterization both qualitatively and quantitatively of the distribution of successive displacements. The multifractal approach, thus, a priori provides no information related to the 3-dimensional structure of the swimming path, as the same pattern in successive displacements can be observed in an organism intermittently swimming following a straight or highly convoluted path. The 2 approaches should then rather be regarded as complementary, and can be compared following the relation $D = d + 1 - \xi(2)/2$, where D is the fractal dimension, d is the dimension of the embedding Euclidean space, and $\xi(2)$ is a specific value of the multifractal structure function exponents, $\xi(q)$; see Seuront et al. 2002 for further details.

Turbulence intensities

Turbulence intensities reported for the ocean range from 2.8×10^{-7} to $4.7 \times 10^{-4} \text{ m}^2/\text{s}^3$ (e.g., Peters and Marrasé 2000). While some laboratory-generated turbulence levels are realistic of oceanic conditions, or at least can be found in the oceans at certain locations and/or under certain circumstances, the distribution of turbulence inten-

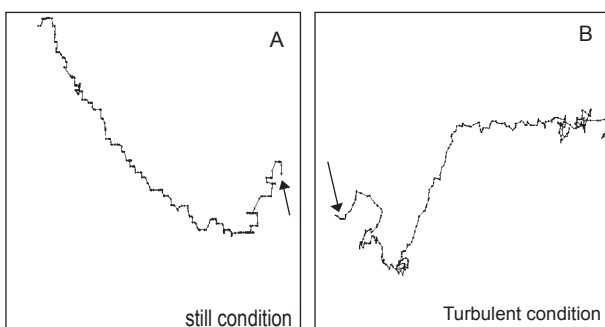


Fig. 8. Examples of 2-D trajectories recorded in still conditions (A) and 1-min exposure to turbulence level 1.

sities that have been reported in laboratory studies has, most of the time, been significantly higher than average values of turbulence reported for oceanic conditions (see Peters and Redondo 1997 for a review; their fig. 4). This is a major concern when extrapolating laboratory results to natural environments. In the present work, the combination of different stroke frequencies and the creation of a clear gradient in the dissipation rates in the "Zoo-Turbularium" (see Fig. 2) led us to consider turbulence intensities ranging very realistically from 3.8×10^{-8} to $1.1 \times 10^{-4} \text{ m}^2/\text{s}^3$. This ensures the reliability of the "Zoo-Turbularium" for turbulence-related studies of zooplankton ecology.

Turbulence and the swimming abilities of *D. pulicaria* and *T. longicornis*

Previous results, based on both theoretical arguments and a literature review (Yamazaki and Squires 1996) or on observations of the swimming ability of free-swimming copepods in a still-water environment (Schmitt and Seuront 2001 2002) have shown that nominal swimming speeds of several zooplankton species (*Euchaeta rimana*, *Oithona davisae*, *Metridia pacifica*, and *T. longicornis*) can exceed micro-scale turbulent velocity fluctuations in most oceanic environments. In this paper, we went a step further in our understanding of the interactions between turbulence and swimming ability on the basis of a novel experimental procedure. We demonstrate that the swimming speed of the cladoceran, *D. pulicaria*, and the calanoid copepod, *T. longicornis*, can overcome velocities by up to 2 and 3 orders of magnitude, respectively, greater than their relative nominal swimming speeds. This indicates that the motion of these 2 organisms can reasonably be regarded as independent of local turbulent flows.

It also must be noted that the 2 species investigated here nevertheless presented significantly different behaviors. We first mention here that escape behavior can be regarded as a directional response to turbulence as it always occurred in the opposite direction of the turbulence gradient. While the number of escape reactions per individual increased with the turbulence level in *D. pulicaria*, it remained constant for *T. longicornis* (Fig. 6A, B). This result made us consider that the hydrodynamic disturbance related to increased turbulence did not affect the swimming behavior of *T. longicornis*. However, the percentage of *Temora* individuals exhibiting escape reactions increased with decreasing distance from the grid for turbu-

lence levels 2 and 3 (see Fig. 6D). This revealed the sensitivity of *T. longicornis* to hydrodynamic disturbances. Comparison of figs. 6B and 6D nevertheless reveals a differential sensitivity to turbulence between *D. pulicaria* and *T. longicornis*. In addition, the differential responses of *D. pulicaria* and *T. longicornis* to light in still conditions (see Fig. 7A, D) demonstrated a stronger phototactic response in the former species.

We finally stress that these differences can reasonably be thought of as consequences of the hydrodynamic properties of the habitats of *D. pulicaria* and *T. longicornis*. The former is found in relatively quiet fresh waters (i.e., ponds, pools, lakes, and river marshes), while the latter is found in coastal waters subjected to strong tidal forcing worldwide. Differences in hydrodynamic regimes between these 2 environments result in differences in dissipation rates of 2 to 5 orders of magnitude. The different behaviors observed in these 2 species, including the considerable ability of *T. longicornis* to adjust its swimming speed to different forcing conditions (Fig. 7D~F) can then be regarded as species-specific properties. In particular, swimming and feeding are fully intertwined in calanoid copepods, and the constant swimming speed exhibited by *T. longicornis* regardless of the intensity of the horizontal velocity gradient may be a way to maintain constant encounter rates with potential prey.

Finally, we stress that the observed patterns are suited to the strongly intermittent nature of oceanic turbulence and allow *T. longicornis* to utilize the benefits of enhanced encounter rates, while minimizing the expense of unnecessary escape responses. While further work is still needed to untangle the complex effects of turbulence on zooplankton behavior, the behavior exhibited by *T. longicornis*, together with the observed differences to those of *D. pulicaria* reveal that this species is fully adapted to highly turbulent environments.

Turbulence intermittency and *D. pulicaria* swimming behavior

To our knowledge, this paper provides the 1st empirical attempt to investigate the effect of turbulence intermittency on zooplankton behavior using free-swimming animals, and the 1st fractal characterization of *D. pulicaria* swimming pathways. The way we experimentally simulated turbulence intermittency might be considered an oversimplification of intermittent events, as they are likely to be

shorter than 1 min (see e.g., Seuront et al. 2001). Despite the extreme character of the turbulent forcing considered here, we nevertheless stress that our results can at least be qualitatively representative of the behavioral response of zooplankton to a localized turbulent patch. We thus showed that the complexity (i.e., the fractal dimension, D) of the swimming paths increased with increasing turbulence intensity (Fig. 9). After a short (1-min) exposure to a turbulence patch, an animal took between 3 and 5 min to recover to its normal (i.e., non-turbulent) swimming behavior, depending on the turbulence intensity. This result is conceptually convergent with the time course of the response to turbulence by a copepod (Costello et al. 1990), showing a “hysteresis-like” effect. Herein, the proposed time scales were bounded between 3 and 5 min. They are comparable with the 6–7 min characteristic of the above-mentioned hysteretic cycle.

This finding has several potential consequences for zooplankton ecology. First, a change in swimming paths implies changes in the hydrodynamic signals generated by the organism, and

therefore of its delectability by a predator. In particular, the behavioral shift observed from smooth, linear swimming paths to more-complex, curvy paths following a turbulence disturbance is associated with increased predation risk via increased hydrodynamic conspicuousness. Turbulence intermittency should then be detrimental to zooplankton. Second, as stated above, swimming and feeding behaviors are closely related. We thus stress that the behavioral changes induced by a burst of turbulence (i.e., an increase in the complexity of the swimming path) may also have some implications on zooplankton trophodynamics. Indeed, if one considers that (i) phytoplankton prey are more homogeneously distributed within a turbulence patch (i.e., their fractal dimension increases with turbulence intensity; Seuront and Schmitt 2001) and (ii) zooplankton predators have less detection ability because of an increase in hydrodynamic ambient noise (e.g., Yamazaki 1993), predation efficiency should be relatively better, because the available food quantity or the encounter rate becomes proportional to the searched volume as the fractal dimension increas-

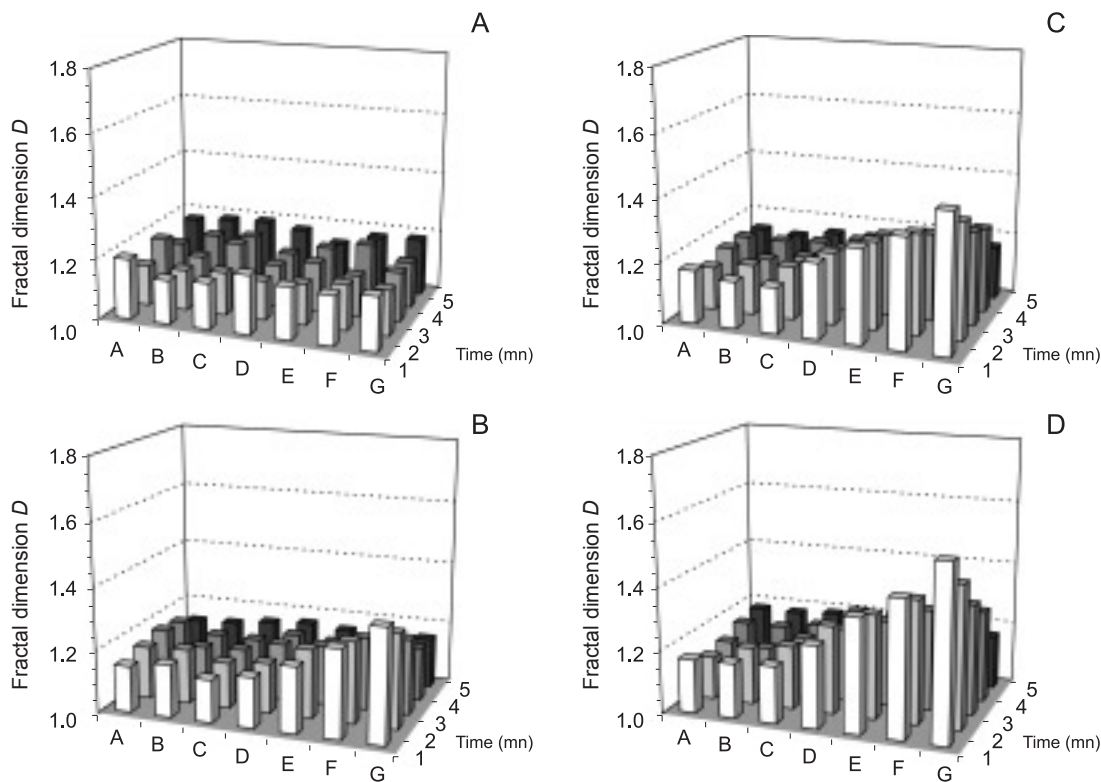


Fig. 9. Fractal dimensions of the swimming paths of *Daphnia pulicaria*, shown as a function of test areas A to G (i.e., decreasing distance from the grid oscillation) and the elapsed time after being kept for 1 min in a given test area under non-turbulent conditions (A) and turbulence levels 1 (B), 2 (C), and 3 (D).

es (Seuront and Lagadeuc 2001).

Finally, while further studies are needed to generalize the present work to different zooplankton species, and to untangle both the qualitative and quantitative nature of biophysical couplings, we state that such approaches may help bridge the gap between empirical work involving zooplankton trophodynamics, and modeling attempts devoted to incorporating individual behavior (Souissi et al. 2004).

Acknowledgments: The authors are indebted to Dr. K. Sakai (Tokyo Univ. of Fisheries, Japan) for providing the *Daphnia pulex* individuals and to Dr. Y. Tanaka (Tokyo Univ. of Fisheries, Japan) for fruitful discussions and his priceless help in untangling linguistic and social situations. We enjoyed our conversations with J. R. Strickler and acknowledge his constructive comments on the manuscript as well as his kind improvement of the language. Thanks are also extended to S. Leterme for her help in the final formatting of the manuscript, and to 2 anonymous reviewers whose comments and suggestions greatly improved the manuscript. A part of this work was supported by a postdoctoral fellowship from the Japan Society for the Promotion of Science and a Monbusho Grant-in-Aid for JSPS Fellows (no. 99756) to L. Seuront. This paper is a contribution of the Ecosystem Complexity Research Group.

REFERENCES

- Brewer MC. 1996. *Daphnia* swimming behavior and its role in predator-prey interactions. PhD thesis, Univ. of Wisconsin-Milwaukee, 155 pp.
- Bundy MH, TF Gross, DJ Coughlin, JR Strickler. 1993. Quantifying copepod searching efficiency using swimming pattern and perceptive ability. *Bull. Mar. Sci.* **53**: 15-28.
- Buskey EJ, PH Lenz, DK Hartline. 2002. Escape behavior of planktonic copepods in response to hydrodynamic disturbances: high-speed video analysis. *Mar. Ecol.-Prog. Ser.* **235**: 135-146.
- Costello JH, JR Strickler, C Marrasé, G Trager, R Zeller, AJ Freise. 1990. Grazing in a turbulent environment: behavioral response of a calanoid copepod, *Centropages hamatus*. *Proc. Natl. Acad. Sci. USA* **87**: 1648-1652.
- Coughlin DJ, JR Strickler, B Sanderson. 1992. Swimming and search behaviour in clownfish, *Amphiprion perideraion*, larvae. *Anim. Behav.* **44**: 427-440.
- Dowling NA, SJ Hall, JG Mitchell. 2000. Foraging kinematics of barramundi during early stages of development. *J. Fish Biol.* **57**: 337-353.
- Fields DM, J Yen. 1997. Implications of the feeding current structure of *Euchaeta rimana*, a carnivorous pelagic copepod, on the spatial orientation of their prey. *J. Plankton Res.* **19**: 79-95.
- Hwang JS, JH Costello, JR Strickler. 1994. Copepod grazing in turbulent flow: elevated foraging behavior and habituation to escape responses. *J. Plankton Res.* **16**: 421-431.
- Jonsson PR, M Johansson. 1997. Swimming behaviour, patch exploitation and dispersal capacity of a marine benthic ciliate in flume flow. *J. Exp. Mar. Biol. Ecol.* **215**: 135-153.
- Kjørboe T. 1997. Small-scale turbulence, marine snow formation, and planktivorous feeding. *Sci. Mar.* **61**: 141-158.
- Kjørboe T, E Saiz. 1995. Planktivorous feeding in calm and turbulent environments, with emphasis on copepods. *Mar. Ecol. Prog. Ser.* **122**: 135-145.
- Loehle C. 1990. Home range: a fractal approach. *Landscape Ecol.* **5**: 39-52.
- Mandelbrot B. 1983. *The fractal geometry of nature*. New York: Freeman.
- Marrasé C, JH Costello, T Granata, JR Strickler. 1990. Grazing in a turbulent environment: energy dissipation, encounter rates, and efficacy of feeding currents in *Centropages hamatus*. *Proc. Natl. Acad. Sci. USA* **87**: 1653-1657.
- Marrasé C, E Saiz, JM Redondo, eds. 1997. Lectures notes on plankton and turbulence. *Sci. Mar.* **61**: 1-238.
- Peters F, C Marrasé. 2000. Effects of turbulence on plankton: an overview of experimental evidence and some theoretical considerations. *Mar. Ecol.-Prog. Ser.* **205**: 291-306.
- Peters F, JM Redondo. 1997. Turbulence generation and measurement: application to studies on plankton. *Sci. Mar.* **61**: 205-228.
- Saiz E, M Alcaraz. 1992. Free-swimming behaviour of *Acartia clausi* (Copepoda: Calanoida) under turbulence water movement. *Mar. Ecol.-Prog. Ser.* **80**: 229-236.
- Saiz E, M Alcaraz. 1992. Enhanced excretion rates induced by small-scale turbulence in *Acartia* (Copepoda: Calanoida). *J. Plankton Res.* **14**: 681-689.
- Saiz E, M Alcaraz, GA Paffenhöffer. 1992. Effects of small-scale turbulence on feeding rate and gross-growth efficiency of three *Acartia* species (Copepoda: Calanoida). *J. Plankton Res.* **14**: 1085-1097.
- Scheirer CJ, WS Roy, N Hare. 1976. The analysis of ranked data derived from completely randomized factorial designs. *Biometrics* **32**: 429-434.
- Schmitt FG, L Seuront. 2001. Multifractal random walk in copepod behavior. *Physica A* **301**: 375-396.
- Schmitt FG, L Seuront. 2002. Diffusion anormale multifractale dans le comportement natatoire d'organismes marins. *In* Y Pomeau, R Ribotta, eds. *Actes de la 5^{ème} Rencontre du Non-linéaire*, Paris, Institut Poincaré. Paris: Non-linéaire publications, pp. 237-242.
- Seuront L. 2001. Microscale processes in the ocean: Why are they so important for ecosystem functioning? *La Mer* **39**: 1-8.
- Seuront L, MC Brewer, JR Strickler. 2004a. Quantifying zooplankton swimming behavior: the question of scale. *In* L Seuront, PG Strutton, eds. *Handbook of scaling methods in aquatic ecology: measurement, analysis, simulation*. Boca Raton, FL: CRC Press, pp. 333-359.
- Seuront L, V Gentilhomme, Y Lagadeuc. 2002. Small-scale nutrient patches in tidally mixed coastal waters. *Mar. Ecol.-Prog. Ser.* **232**: 29-44.
- Seuront L, Y Lagadeuc. 2001. Multiscale patchiness of the calanoid copepod *Temora longicornis* in a turbulent coastal sea. *J. Plankton Res.* **23**: 1137-1145.
- Seuront L, FG Schmitt. 2001. Describing intermittent processes in the ocean-Univariate and bivariate multiscaling procedures. *In* P Muller, C Garrett, eds. *Stirring and mixing in a stratified ocean*. Proc. of "Aha Huliko" a Hawaiian

- Winter Workshop, SOEST, Univ. of Hawaii, pp. 129-144.
- Seuront L, FG Schmitt, MC Brewer, JR Strickler, S Souissi. 2004b. From random walk to multifractal random walk in zooplankton swimming behavior. *Zool. Stud.* **43**: 498-510.
- Seuront L, F Schmitt, Y Lagadeuc. 2001. Turbulence intermittency, small-scale phytoplankton patchiness and encounter rates in plankton: Where do we go from here? *Deep-Sea Res. PT I* **48**: 1199-1215.
- Siegel S, NJ Castellán. 1988. Non parametric statistics for the behavioral sciences. New York: McGraw Hill.
- Singarajah KV. 1969. Escape reactions of zooplankton: the avoidance of pursuing copepods. *J. Exp. Mar. Biol. Ecol.* **3**: 171-178.
- Sokal RR, FJ Rohlf. 1995. Biometry. New York: Freeman.
- Souissi S, V Ginot, L Seuront, SI Uye. 2004. Using multi-agent systems to develop individual based models for copepods: consequences of individual behaviour and spatial heterogeneity on the emerging properties at the population scale. *In* L Seuront, PG Strutton, eds. Scales in aquatic ecosystems: measurement, analysis, simulations. Boca Raton, FL: CRC Press, pp. 523-542.
- Stiansen JE, S Sundby. 2001. Improved methods for generating and estimating turbulence in tanks suitable for fish larvae experiments. *Sci. Mar.* **65**: 151-167.
- Suchman CL. 2000. Escape behavior of *Acartia hudsonica* copepods during interactions with scyphomedusae. *J. Plankton Res.* **22**: 2307-2323.
- Taylor GI. 1935. Statistical theory of turbulence. *Proc. R. Soc. London Ser. A* **151**: 1-421.
- Tennekes H. 1975. Eulerian and Lagrangian time microscales in isotropic turbulence. *J. Fluid Mech.* **67**: 561-567.
- Thompson SM, JS Turner. 1975. Mixing across an interface due to turbulence generated by an oscillating grid. *J. Fluid Mech.* **67**: 349-368.
- Van Gool E, J Ringelberg. 2002. Relationship between fish kairomone concentration in a lake and phototactic swimming by *Daphnia*. *J. Plankton Res.* **24**: 713-721.
- Voss RF. 1988. Fractals in nature: from characterization to simulation. *In* HO Peitgen, D Saupe, eds. The science of fractal images. New York: Springer, pp. 21-70.
- Yamazaki H. 1993. Lagrangian study of planktonic organisms: perspectives. *Bull. Mar. Sci.* **53**: 265-278.
- Yamazaki H, KD Squires. 1996. Comparison of oceanic turbulence and copepod swimming. *Mar. Ecol.-Prog. Ser.* **144**: 299-301.